



Modeling and Reduction of Shocks on Electronic Components Within a Projectile

**by Vinod Chakka, Mohamed B. Trabia, Brendan O'Toole,
Srujanbabu Sridharala, Samaan Ladkany, and Mostafiz Chowdhury**

ARL-RP-217

August 2008

A reprint from the *International Journal of Impact Engineering*, vol. 35, pp. 1326–1338, 2008.

NOTICES

Disclaimers

The findings in this report are not to be construed as an official Department of the Army position unless so designated by other authorized documents.

Citation of manufacturer's or trade names does not constitute an official endorsement or approval of the use thereof.

Destroy this report when it is no longer needed. Do not return it to the originator.

Army Research Laboratory

Adelphi, MD 20783-1197

ARL-RP-217

August 2008

Modeling and Reduction of Shocks on Electronic Components Within a Projectile

**Vinod Chakka, Mohamed B. Trabia, Brendan O'Toole,
Srujanbabu Sridharala, and Samaan Ladkany
University of Nevada**

**Mostafiz Chowdhury
Weapons and Materials Research Directorate, ARL**

A reprint from the *International Journal of Impact Engineering*, vol. 35, pp. 1326–1338, 2008.

REPORT DOCUMENTATION PAGE			Form Approved OMB No. 0704-0188		
Public reporting burden for this collection of information is estimated to average 1 hour per response, including the time for reviewing instructions, searching existing data sources, gathering and maintaining the data needed, and completing and reviewing the collection information. Send comments regarding this burden estimate or any other aspect of this collection of information, including suggestions for reducing the burden, to Department of Defense, Washington Headquarters Services, Directorate for Information Operations and Reports (0704-0188), 1215 Jefferson Davis Highway, Suite 1204, Arlington, VA 22202-4302. Respondents should be aware that notwithstanding any other provision of law, no person shall be subject to any penalty for failing to comply with a collection of information if it does not display a currently valid OMB control number. PLEASE DO NOT RETURN YOUR FORM TO THE ABOVE ADDRESS.					
1. REPORT DATE (DD-MM-YYYY) August 2008		2. REPORT TYPE Reprint		3. DATES COVERED (From - To) January 2005–January 2007	
4. TITLE AND SUBTITLE Modeling and Reduction of Shocks on Electronic Components Within a Projectile				5a. CONTRACT NUMBER	
				5b. GRANT NUMBER	
				5c. PROGRAM ELEMENT NUMBER	
6. AUTHOR(S) Vinod Chakka,* Mohamed B. Trabia,* Brendan O’Toole,* Srujanbabu Sridharala,* Samaan Ladvany,† and Mostafiz Chowdhury				5d. PROJECT NUMBER DAAD19-03-2-0007	
				5e. TASK NUMBER	
				5f. WORK UNIT NUMBER	
7. PERFORMING ORGANIZATION NAME(S) AND ADDRESS(ES) U.S. Army Research Laboratory ATTN: AMSRD-ARL-WM-MB Adelphi, MD 20783-1197				8. PERFORMING ORGANIZATION REPORT NUMBER ARL-RP-217	
9. SPONSORING/MONITORING AGENCY NAME(S) AND ADDRESS(ES)				10. SPONSOR/MONITOR'S ACRONYM(S)	
				11. SPONSOR/MONITOR'S REPORT NUMBER(S)	
12. DISTRIBUTION/AVAILABILITY STATEMENT Approved for public release; distribution is unlimited.					
13. SUPPLEMENTARY NOTES A reprint from the <i>International Journal of Impact Engineering</i> , vol. 35, pp. 1326–1338, 2008. *Department of Mechanical Engineering, University of Nevada, Las Vegas, NV 89154-4027 †Department of Civil and Environmental Engineering, University of Nevada, Las Vegas, NV 89154-4027					
14. ABSTRACT Electronic components within a projectile are subjected to severe loads over an extremely short duration during the launch process. Failure of these components during launch can result in negative effects on the mission of the projectile. While experimental data can be helpful in understanding failure of electronic components within a projectile, collecting such data are [<i>sic</i>] usually difficult. There are also limitations on the reliability of sensors under these circumstances. Finite element modeling (FEM) can offer a means to better understand the behavior of these components. It can also be used to develop better shock mitigation features into the projectile design. This research has two objectives. The first objective is to develop an FEM that one describes the interaction of a typical projectile with the gun barrel during launch. The projectile includes a payload of a one-pound mass representing a typical electronic package supported by a plate. The second objective of this work is to investigate the use of composite plates to support electronic payload as a means to reduce the transmitted shocks during the projectile launch event. The proposed plate has carbon fibers embedded in an epoxy matrix. A parametric study of the effects of varying the thickness of the supporting plate and the fiber volume fraction on the accelerations and stresses is included. Results of the study are used to reach general recommendations regarding reducing failure of electronic components within a projectile.					
15. SUBJECT TERMS projectile, finite element modeling, electronic component, shock, composites					
16. SECURITY CLASSIFICATION OF:			17. LIMITATION OF ABSTRACT UL	18. NUMBER OF PAGES 24	19a. NAME OF RESPONSIBLE PERSON Mostafiz R. Chowdhury
a. REPORT UNCLASSIFIED	b. ABSTRACT UNCLASSIFIED	c. THIS PAGE UNCLASSIFIED			19b. TELEPHONE NUMBER (Include area code) (301) 394-6308

Modeling and reduction of shocks on electronic components within a projectile

Vinod Chakka^a, Mohamed B. Trabia^{a,*}, Brendan O'Toole^a, Srujanbabu Sridharala^a,
Samaan Ladkany^b, Mostafiz Chowdhury^c

^aDepartment of Mechanical Engineering, University of Nevada, Las Vegas, Las Vegas, NV 89154-4027, USA

^bDepartment of Civil and Environmental Engineering, University of Nevada, Las Vegas, Las Vegas, NV 89154-4027, USA

^cAMSRL-WM-MB (ALC), Ordnance Materials Branch, Weapons & Materials Research Directorate, US Army Research Laboratory, 2800 Powder Mill Road, Adelphi, MD 20783-1145, USA

Received 16 October 2006; received in revised form 12 January 2007; accepted 24 July 2007

Available online 3 August 2007

Abstract

Electronic components within a projectile are subjected to severe loads over an extremely short duration during the launch process. Failure of these components during launch can result in negative effects on the mission of the projectile. While experimental data can be helpful in understanding failure of electronic components within a projectile, collecting such data are usually difficult. There are also limitations on the reliability of sensors under these circumstances. Finite element modeling (FEM) can offer a means to better understand the behavior of these components. It can also be used to develop better shock mitigation features into the projectile design. This research has two objectives. The first objective is to develop an FEM that one describes the interaction of a typical projectile with the gun barrel during launch. The projectile includes a payload of a one-pound mass representing a typical electronic package supported by a plate. The second objective of this work is to investigate the use of composite plates to support electronic payload as a means to reduce the transmitted shocks during the projectile launch event. The proposed plate has carbon fibers embedded in an epoxy matrix. A parametric study of the effects of varying the thickness of the supporting plate and the fiber volume fraction on the accelerations and stresses is included. Results of the study are used to reach general recommendations regarding reducing failure of electronic components within a projectile.

© 2007 Elsevier Ltd. All rights reserved.

Keywords: Projectile; Modeling; Shock; Finite element; Electronic components

1. Introduction

During the last thirty years, the US Army has been developing “smart artillery” munitions, which contain sophisticated embedded electronic systems. Unfortunately, the artillery environment is extremely harsh as the munitions must operate in temperatures ranging from -60°F to 160°F . The projectiles are subjected to quasi-static axial loads in excess of 15,000 g during the launch

process which is augmented by transient loads of up to 5000 g at the muzzle exit [1]. Projectiles can also spin at up to 300 revolutions per second. As a projectile travels down the gun barrel, it may also be subject to off-axis loads from impacts with the gun tube walls caused by balloting [2].

Heaslip and Punch [3] concluded that there is considerable evidence to suggest that a large percentage of portable electronic products fail due to impact or shock during use. Some of the electronic component failure problems can be reduced by enclosing the components within foam. This approach, however, reduces the requirement that the electronic components should also be upgradeable and replaceable without swapping an entire subsystem of the projectile. These challenges present significant problems for designers who typically resort to the use of numerical

*Corresponding author. Tel.: +1 702 895 0957; fax: +1 702 895 3936.

E-mail addresses: vinod_engg1@yahoo.com (V. Chakka), mbt@me.unlv.edu (M.B. Trabia), bj@me.unlv.edu (B. O'Toole), srujanbabus@yahoo.com (S. Sridharala), samaan@ce.unlv.edu (S. Ladkany), MChowdhury@arl.army.mil (M. Chowdhury).

simulations to provide guidance on these complex design issues.

One of the difficulties facing the US Army and its contractors is identifying the correct gun launch loads to electronic component manufacturers prior to the final design of the projectile. In the past, pressure–time curves and peak acceleration values were provided to contractors. Contractors used the peak values to perform static analysis and quasi-static in centrifuge tests. The dynamics of the projectile structure [3], particularly during the muzzle exit transient, were usually neglected. As a result, programs like the US Army's Excalibur and SADARM experienced numerous failures of sensitive equipment during the early stages of development. Failure of several sensitive components was traced to the muzzle exit event in the Excalibur program [4].

Few researchers considered creating a fully detailed model of a projectile launch event. This research has two objectives:

- Develop a gun-launched projectile finite element model (FEM) capable of predicting shocks transmitted to on-board electronic components during the launch process. The projectile is subjected to a realistic launch pressure–time history. The model includes friction between the gun barrel inner surface and the projectile as well as the flexibility of the gun barrel. The effects of these factors on the vibrations of the electronic package are also considered.
- Investigate the effects of composite laminate parameters on reducing the transmitted shocks to embedded electronic components through passive damping.

The following is a review of relevant research. Simkins et al. [5] studied dynamics of gun tubes, especially interaction between strains in the wall of the gun tube and projectile velocity to predict resonant conditions. Hopkins and Wilkerson [6] examined the results of a series of experiments conducted in an attempt to reduce the dynamic motions of the M256 gun system during firing. Data collected during these experiments included the motion of the gun tube and breech mechanism. An axisymmetric transient FEM of the entire system was developed and used to explain the experimental results. Hollis [7] developed a two-dimensional quasi-static model of a training projectile. The projectile was redesigned to reduce stresses. Cordes et al. [2] presented a simplified model of a projectile using shell elements. Natural frequency effects were considered in this model. Kessler and Spearing [8] studied an autonomous flying vehicle that is launched from an artillery shell, and then deployed over a battlefield to capture images. They developed the structural design and testing of the aft section of this vehicle, which is subjected to high impulsive inertial loads. A quasi-dynamic FEM of the aft section was developed whose results were compared with launch data. Chowdhury et al. [1] successfully used a 3D FE gun-launch simulation model—including balloting, spinning, and gun

mount positioning—of a surrogate Excalibur projectile in support of its design development. In their paper, the impacts of an FEM in locating trouble-free mounting locations for sensitive electronic components and the need for parametric study in identifying sensitive factors affecting the muzzle exit dynamics of projectile was demonstrated. Petersen [9] proposed a test pan to gather information on the dynamics of the 155-mm Advanced Gun System barrel as a projectile travels down the gun tube to corroborate modeling efforts using sensors on the gun barrel to measure the position, acceleration, and strain during firing. The acquired data are compared to barrel-projectile interaction FEM. Recently, an analytic approach is proposed to investigate the dynamic behavior of laboratory rail guns resulting from launching a projectile [10]. The rail gun is modeled as a beam with an elastic foundation with cantilevered support at the breech end of rails. The analysis showed that structural response of the rail is governed by a transient fourth-order differential equation. Flexibility of the gun was not considered in most of these models.

In addition to developing an accurate model of the projectile and gun barrel, it is important to explore means of reducing transmitted vibrations to electronic payloads. Most of the research in this area concerns the use of smart materials to passively dampen vibrations such as dynamic vibration absorbers or resonant circuit shunted piezoceramics [11]. On the other hand, few researchers considered modifying characteristics of composite structure to passively reduce vibrations. For example, Trindade [12] used genetic algorithms to optimize the geometry of a laminated composite beam for passive damping. None of the surveyed literature addressed the problem of shock loading within a projectile launch event.

The remainder of this paper is divided as follows: Section 2 presents description of the projectile and gun. An FEM for the projectile and gun is developed in Section 3. An approach for the design of the electronic payload supporting composite plate is presented in Section 4. Conclusions and recommendations for future work are listed in Section 5.

2. Description of the projectile and gun

The US Army ARDEC Tank-automotive & Armaments Command-Armaments Research, Development & Engineering Center (TACOM-ARDEC) provided the data for the projectile under consideration, using an instrumented projectile, Fig. 1(a), to collect data within and outside the gun including pressure and acceleration time histories. The projectile is composed of several components: M795 Body, ogive, nacelle, and windshield. All these components are threaded into each other or bolted together. A band on the M795 maintains contact between the projectile and the walls of the gun. The properties for all parts are listed in Tables 1 and 2. The actual projectile has various electronic components occupying its top half in addition to pressure

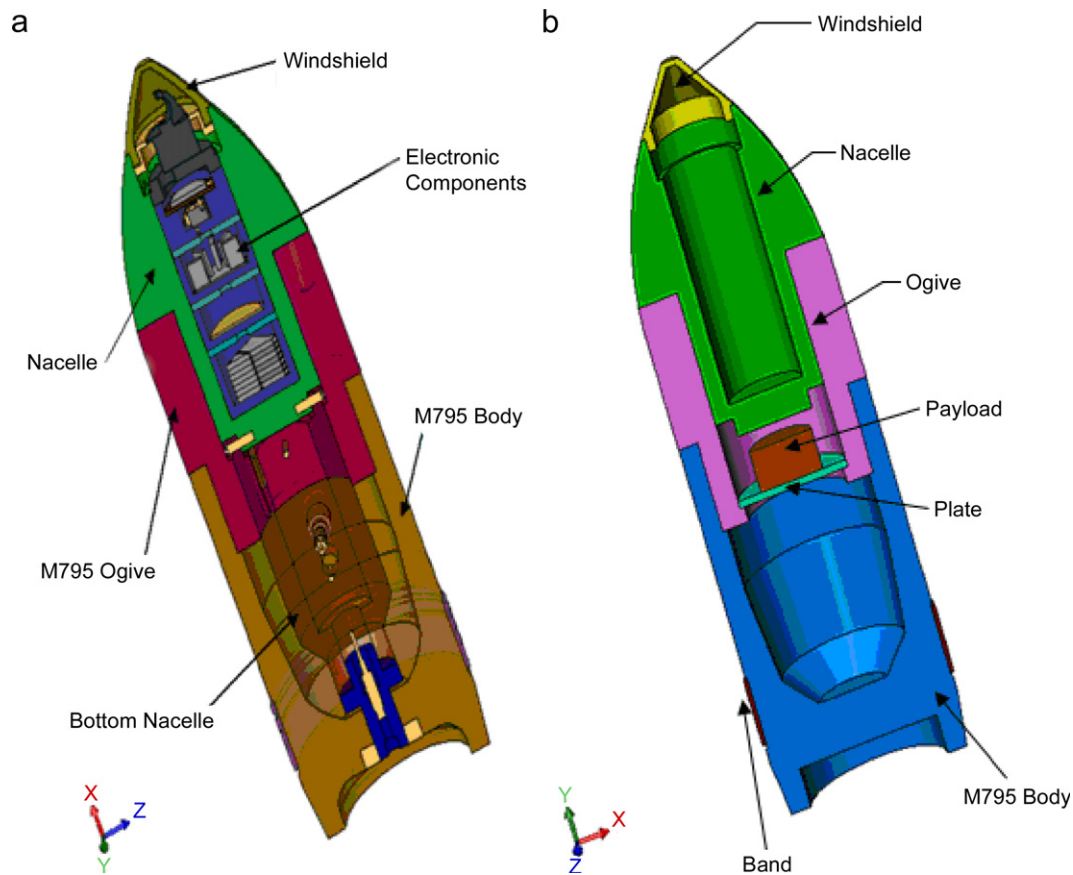


Fig. 1. Sectional view of the original projectile and its simplified model.

Table 1
Material properties of projectile parts and gun barrel

Part name	Material	Specific weight (lbf/in ³)
Wind shield	Ultem 2300 (30% glass)	0.055
Nacelle	Aluminum 7075-T6511	0.103
Ogive, M795, plate, payload, band, gun barrel	4030 Steel	0.283

transducers at the bottom and mid-section of the projectile to measure axial and radial pressures. The modeling was simplified by eliminating the exact details of all the electronic components and focusing on the response of a single generic electronic component. Based on suggestions of TACOM-ARDEC, it was decided to eliminate these electronic components and to adjust the mass of nacelle accordingly. A one-pound mass, which corresponds to a typical electronic package, is added as shown in Fig. 1(b). This payload is supported by a steel plate that is fully attached to the Ogive (Fig. 1(b)). The thickness of this plate is similar to what is typically used in industry. Critical dimensions of the projectile are shown in Fig. 2. The inner

diameter of the Ogive is slightly reduced to provide an attachment point for the plate. The maximum diameter of the projectile is 6.22 in. at the band, which is equal to the inner diameter of the gun barrel. The total height of the projectile is 20.5 in. The gun barrel is modeled as a long hollow cylindrical tube. The inside and outside diameters of the gun barrel are 6.22 and 11.62 in, respectively. The total length of the gun barrel is 264 in. The gun barrel is supported by two bearings at 10 and 40 in. from the bottom of the gun barrel (breech of the gun) as shown in Fig. 3. The gun barrel model used in the simulation is a simplification of the actual gun tube considering that the bore evacuator has an effect on launch dynamics [13].

3. Development of the FEM

3.1. Meshing

LS-Dyna [14] is used to simulate the motion of the projectile. Most components of the projectile, except for the base of the M795 Body, the payload, and the support plate, are modeled by creating a two-dimensional sketch for each of them. Each sketch is meshed using quadrilateral elements. These sketches are then swept 360° to create corresponding volumes, which are meshed using eight-node brick elements. The two-dimensional mesh is then deleted.

Table 2
Mechanical characteristics of projectile parts and gun barrel

Part name	Young's modulus (psi)	Poisson's ratio	Yield stress (psi)	Tangent modulus (psi)
Wind shield	8.00E+05	0.40	24.5E+03	–
Nacelle	1.04E+07	0.33	68.0E+03	1.85E+04
Ogive, M795, plate, payload, band, gun barrel	2.90E+07	0.32	120E+03	5.21E+04

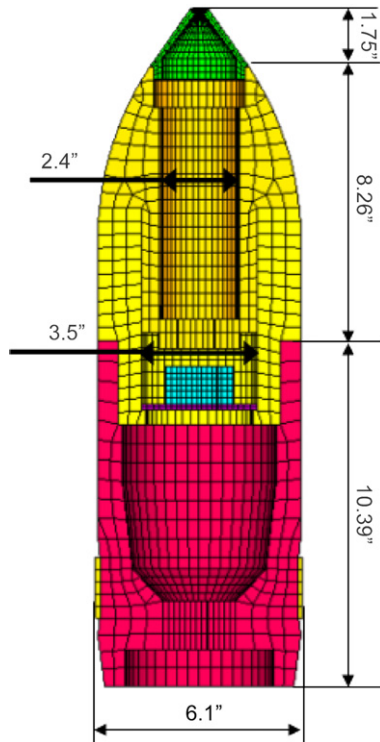


Fig. 2. Sectional view of the meshed projectile model.

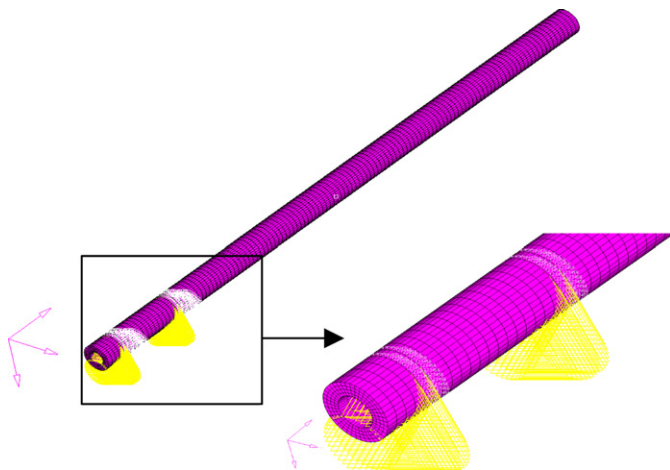


Fig. 3. Meshed gun barrel with boundary conditions applied.

Nodes are merged at the beginning and end of the swept volume to eliminate duplicate nodes. A sectional view of the meshed projectile is shown in Fig. 2.

For the gun tube model, a two-dimensional mesh is created at the base of the gun. This mesh is extruded along the axis of the gun barrel. About 124 layers of eight-node brick elements are created in this way. A similar approach is used to create the base of the M95 Body, the payload, and the support plate. Fig. 3 depicts a meshed gun barrel. All projectile components and gun models have 40 elements in the circumferential direction.

3.2. Loads and boundary conditions

The ballistics of the gun barrel is represented by a high-g impulsive thrust driving the base of the projectile. Fig. 4 shows a typical pressure–time history that was measured at the base of the projectile using the sensor shown in Fig. 1 [1]. Base pressure distributions on the model are shown in Figs. 5 and 6. Gravity load is applied in the negative x -axis of the global frame, Fig. 7.

Interfacing between various contact surfaces within the projectile is defined by selecting a set of elements on each of the two contacting parts that are adjacent to the contact area. The type of contact and the role acted by each part are then introduced. Table 3 summarizes contact definitions between various parts of the model. The coefficient of friction between the gun barrel and the band is set equal to 0.1.

As described in the previous section, the gun barrel is supported by two bearings at 10 and 40 in. from the breech of the gun barrel. These boundary conditions are simulated by identifying a band of elements at each of these two locations. All degrees of freedom for nodes on the outer surface of these two bands, Fig. 3, are constrained.

3.3. Analysis approach

The projectile launch event is modeled in two phases. In the first phase, only the gun barrel is allowed to deflect due to gravity in the negative x -direction. This analysis is conducted for 0.5 s, which allows the gun to reach its static deflection position. Fig. 7 shows the original and deflected gun barrels.

In the second phase of the analysis, the pressure curve of Fig. 4 is applied in a normal direction to all the surfaces of the base portion of the projectile below the band as shown in Figs. 5 and 6. The initial conditions of this phase are obtained from the results of the first phase of the analysis. Gravity load continues to be active in this phase also. The duration of the simulation for the second phase is 0.02 s.

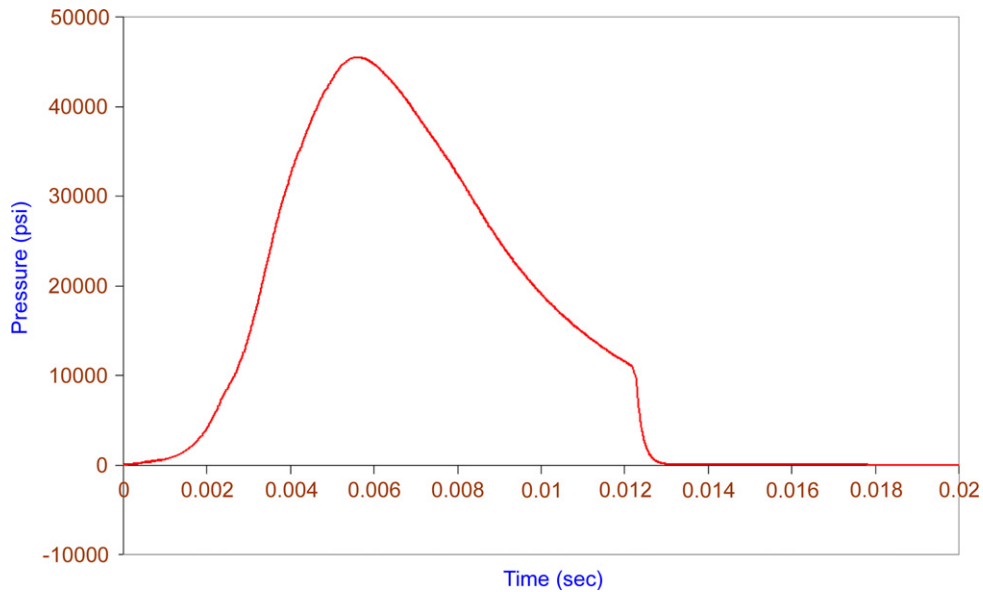


Fig. 4. Projectile pressure curve.

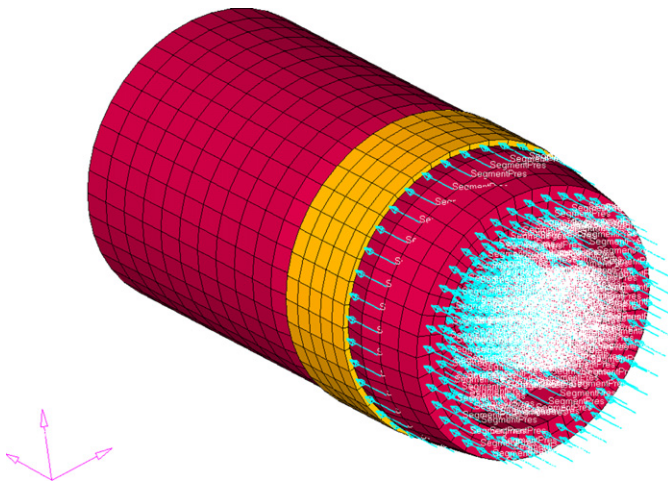


Fig. 5. Pressure loads on the base of M795 and the band.

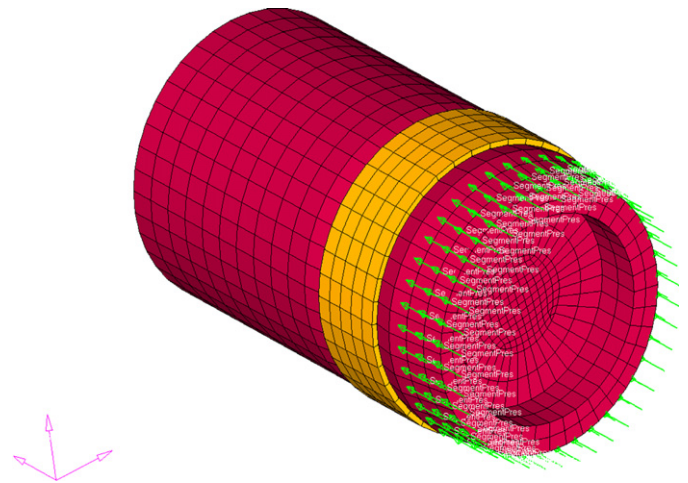


Fig. 6. Pressure loads on the slanted surfaces of M795.

The pressure pushes the projectile through the deformed gun barrel for the first 0.0125 s of this phase. The gun is not internally pressurized as the effect of the pressure is found to be minimal. The initial position of the projectile is chosen to ensure that the lower edge of the band is aligned with the tip of the gun barrel when the pressure curve is first equal to zero (time 0.0125 s after the beginning of the second phase). Several trials result in the conclusion that the bottom of the projectile should be placed at 73 in. from the breech of the gun barrel. Results of the FEM confirm this initial location. Fig. 8 shows the deformed shape of the gun barrel in the x -direction (gravity direction) at various time instants. The figure shows that gravity effects dominate the deformation. However, as the projectile moves inside the gun barrel it slightly straightens the gun.

Acceleration, velocity, and displacement data are recorded for nodes on the payload and the nacelle as shown

in Fig. 9. Fig. 10 shows typical experimental (unfiltered) acceleration results for projectile of the type used in this study. Integrating this curve yields velocity and displacement curves that are close to those shown in Figs. 11 and 12, respectively. However, acceleration results, Figs. 13 and 14, have significantly higher level of noise than what is observed in the experimental results. Increasing the number of elements in the axial, tangential, and radial directions was explored as a means to reduce this acceleration noise in the FEM results. Such approach however produced limited improvement in the results, while proving to be computationally prohibitive.

Acceleration results are therefore filtered. A modal analysis of the projectile is conducted. Modal analysis results are listed in Table 4. Fig. 15 shows the mode shape of the first bending frequency. It is decided to filter acceleration results at a frequency of 6000 Hz. This value is

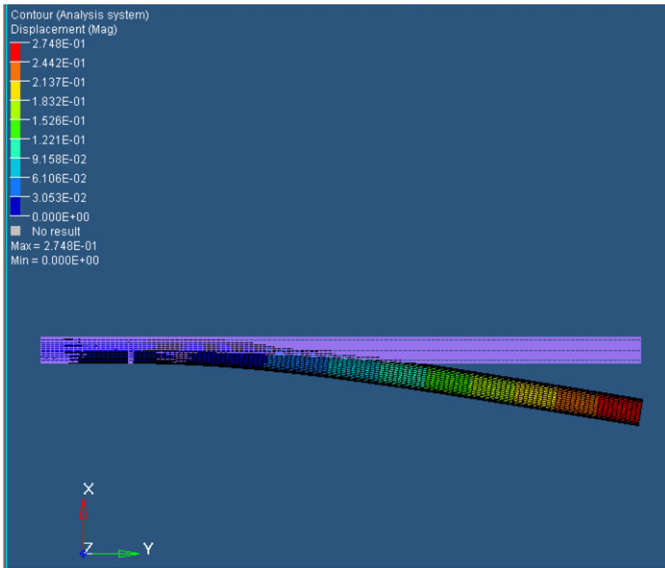
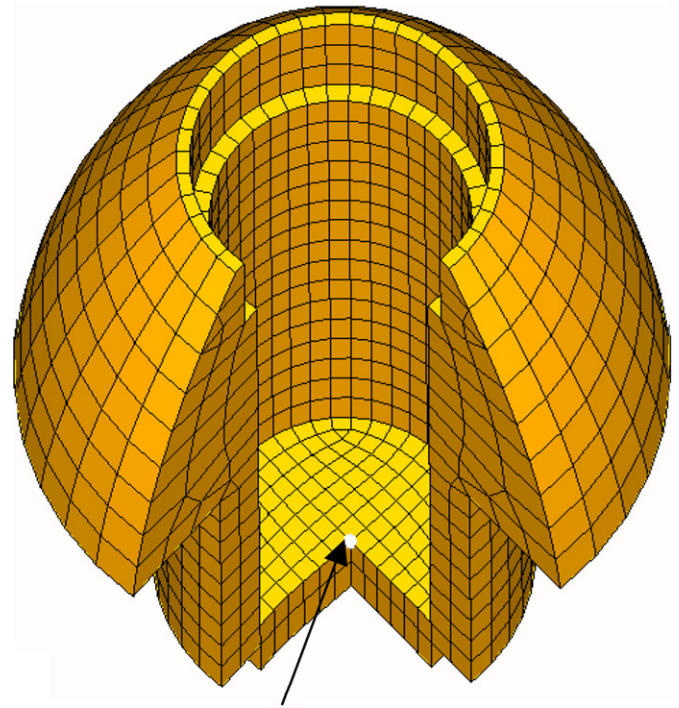


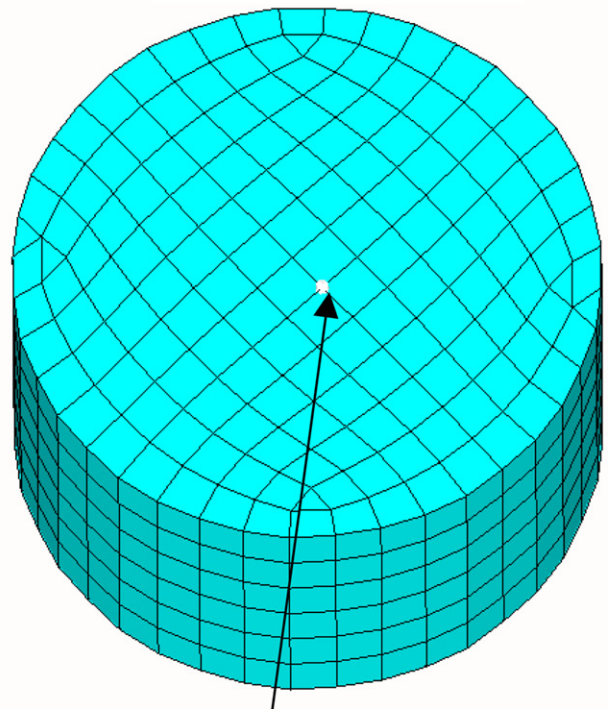
Fig. 7. Static deflection of the gun barrel.

Table 3
Contact characteristics

Master	Slave	Contact type
Nacelle	Windshield	Tied surface to surface
Ogive	Nacelle	Tied surface to surface
Plate	Payload	Tied surface to surface
Ogive	Plate	Tied surface to surface
M795 body	Ogive	Tied surface to surface
Gun barrel	Band	Surface to surface



Node on Projectile



Node on Payload

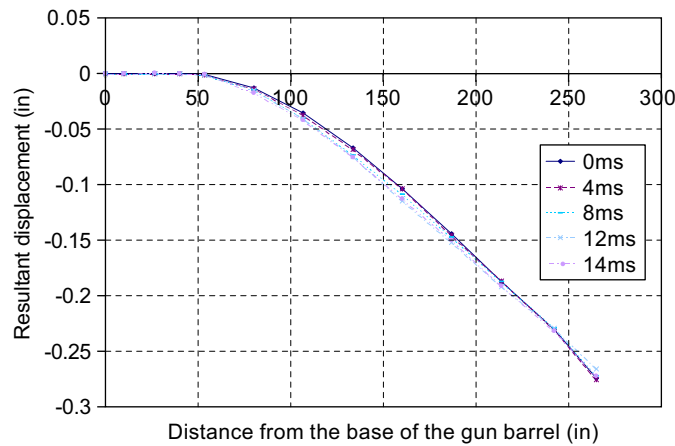


Fig. 8. Deformed shape of the gun barrel in the *x*-direction.

Fig. 9. Locations of data collection.

chosen as it is larger than all major frequencies of the projectile. Figs. 16 and 17 show the filtered accelerations for the same nodes of Figs. 13 and 14, respectively. These results are comparable to those observed in test firing of projectiles. While accelerations of these two nodes are of the same order of magnitude, the payload exhibits significantly lower-order frequencies due to the difference

in stiffness between the projectile and the supporting plate. The results of Fig. 17 also show that the payload experiences accelerations of relatively higher magnitude after the projectile exits the muzzle. This “ringing”

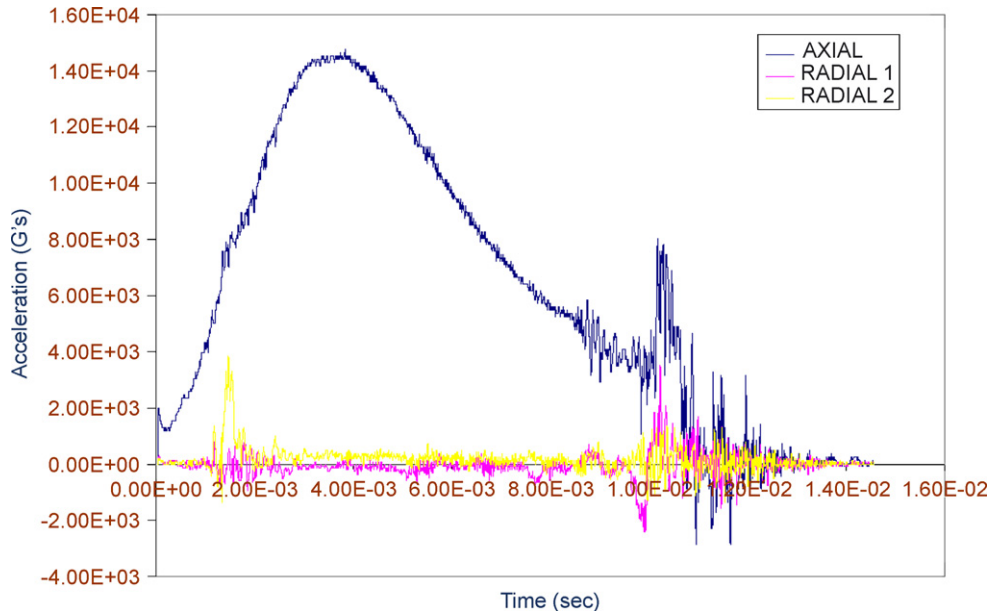


Fig. 10. Typical experimental acceleration curves for a point in the projectile during launch.

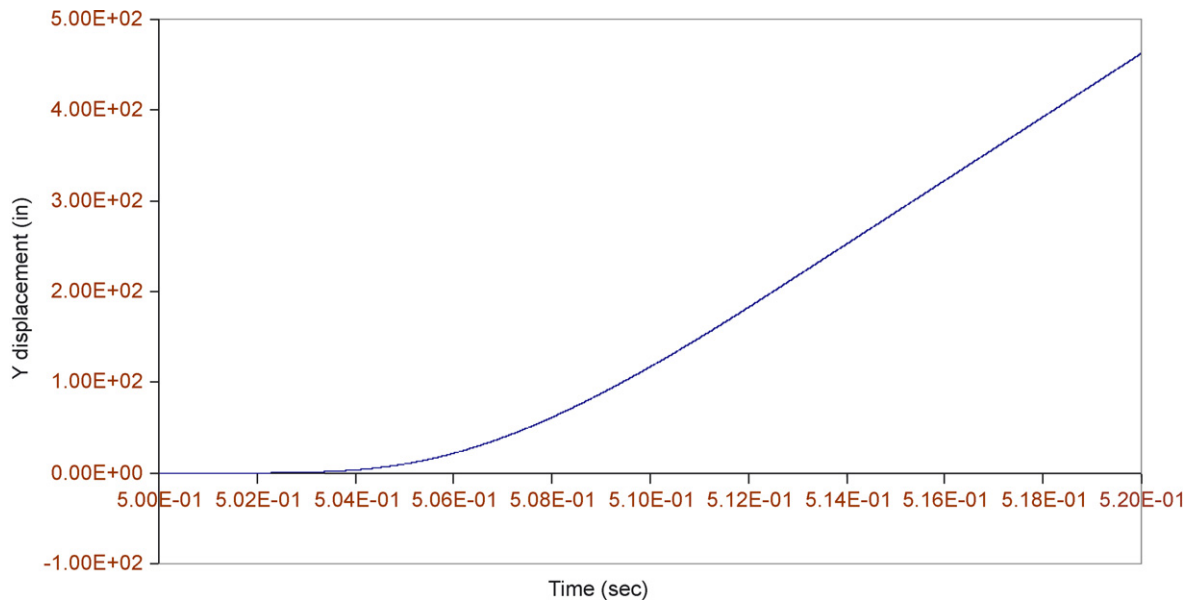


Fig. 11. Axial displacement for a node on the payload.

phenomenon is of special concern to failure of electronic components in this phase.

4. Design of the electronic payload supporting composite plate

The results of the previous section show that accelerations of the electronic payload can be divided into two phases: inside the gun barrel and after muzzle exit. In the first phase, accelerations are governed by the input pressure curve and cannot be seriously affected by

choosing a different supporting plate. In the second phase, the projectile and the electronic payload experience free vibration as the pressure load rapidly disappears. The associated oscillatory accelerations often lead to the failure of these components. Therefore, choosing the appropriate plate characteristics affects the vibration. This is especially important since experimental results reported that failure of electronic components usually occurs immediately after the projectile leaves the gun barrel. A desirable plate performance should combine low peak accelerations and low frequency after the

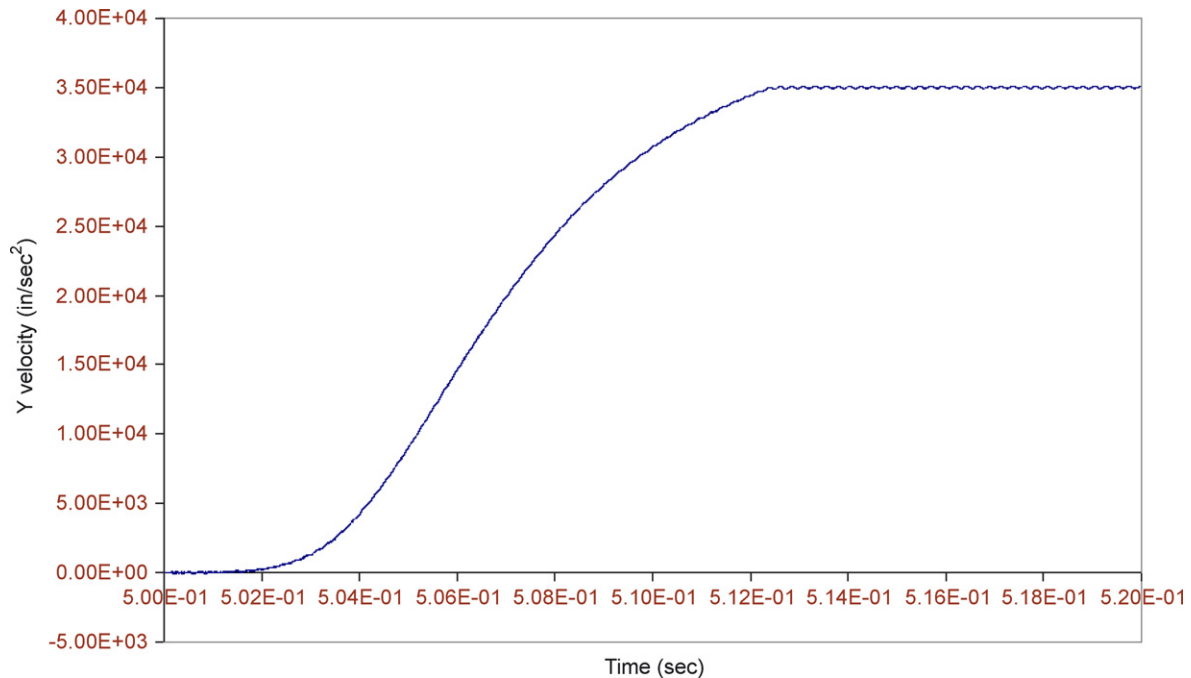


Fig. 12. Axial velocity for a node on the payload.

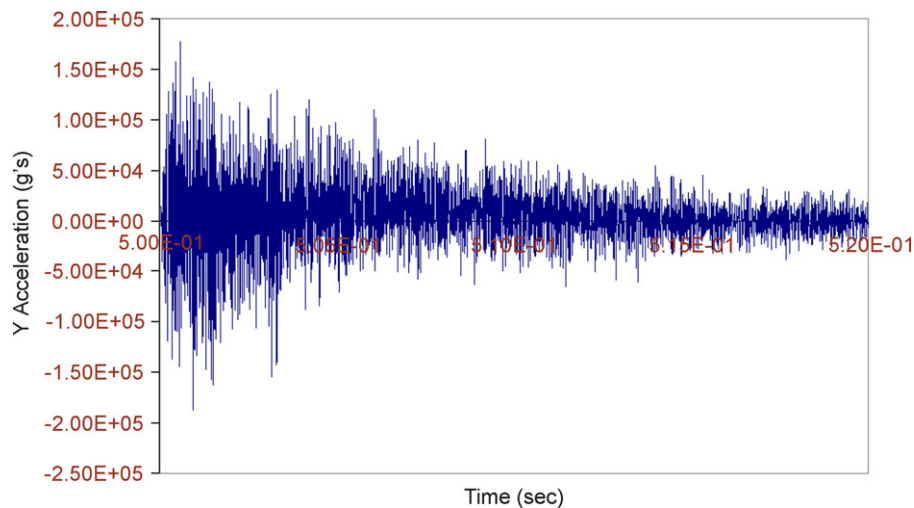


Fig. 13. Axial acceleration for a node on the nacelle/projectile.

projectile leaves the gun to ensure the survivability of the electronic components it carries.

A parametric study to explore the effect of using a composite material plate on reducing the accelerations transmitted to the payload is presented in this section. The plate is made of standard modulus carbon fibers embedded in an epoxy matrix. Three layers are used to create the laminate. Individual fiber and epoxy properties used for the analysis are listed in Table 5. The plate is designed as a quasi-isotropic composite laminate for which material properties are isotropic in plane. It is decided to use a three-laminae composite for the supporting plate. The fiber

orientation angle of the laminae of θ° , 0° , and $-\theta^\circ$, Fig. 18, is suggested in [15] for this type of application. Exploded and stacked views of the three laminae are shown in Fig. 18. Appendix A lists the equations used to calculate the properties of the composite laminate. Solid brick elements are used to model the composite plate. The fiber angle orientation of 60° , 0° , and -60° is used in this work. Ongoing experimental work shows that the characteristics of the supporting plate material are not sensitive to strain rate variations within the current projectile environment [16].

Initially, a composite plate having 30% fiber volume fraction and 0.2 in. plate thickness, which is the same

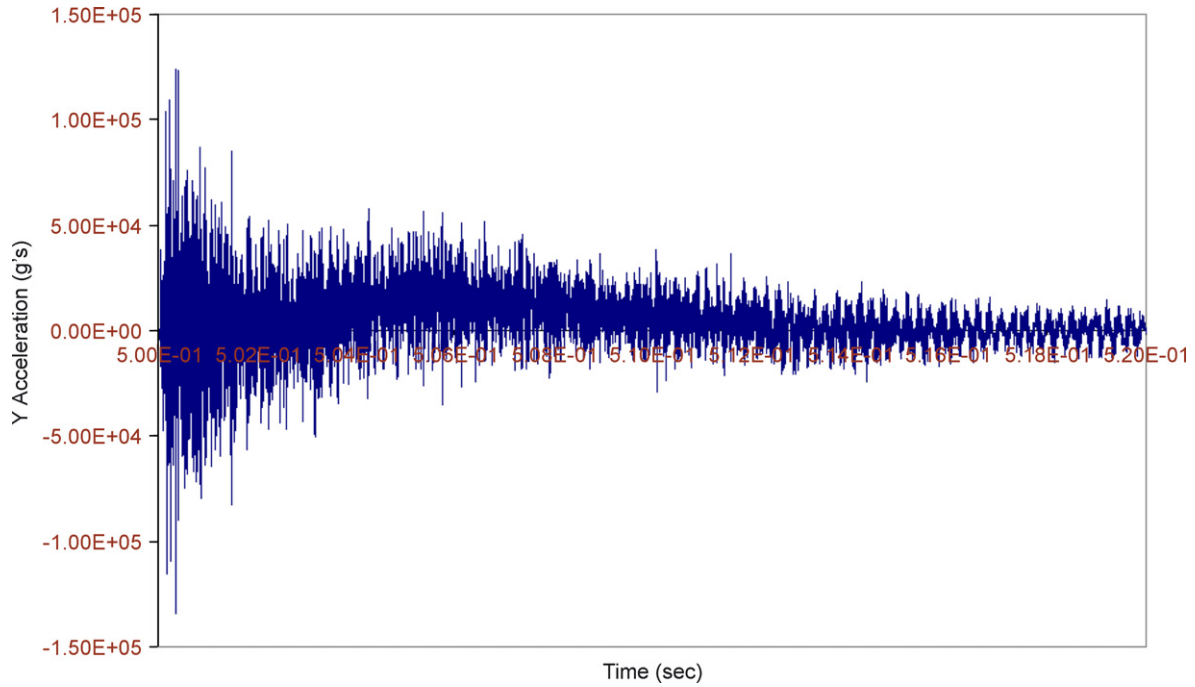


Fig. 14. Axial acceleration for a node on the payload.

Table 4
Modal results of the projectile

Mode number	Frequency (Hz)	Type of mode
1	1786	1st Bending mode of payload and plate
2	1863	2nd Bending mode of payload and plate
3	2008	3rd Bending mode of payload and plate
4	3145	1st Bending mode of the projectile
5	3711	1st Torsional mode of projectile
6	5211	1st Axial mode of the projectile
7	5469	1st Radial mode of the projectile

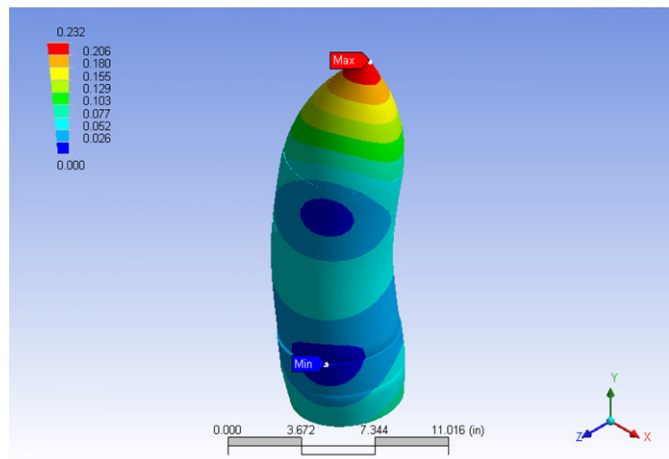


Fig. 15. Mode shape of the first bending frequency of the projectile.

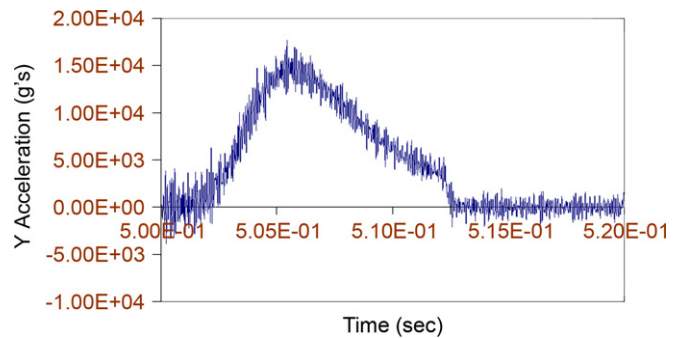


Fig. 16. Filtered axial acceleration for a node on the nacelle/projectile.

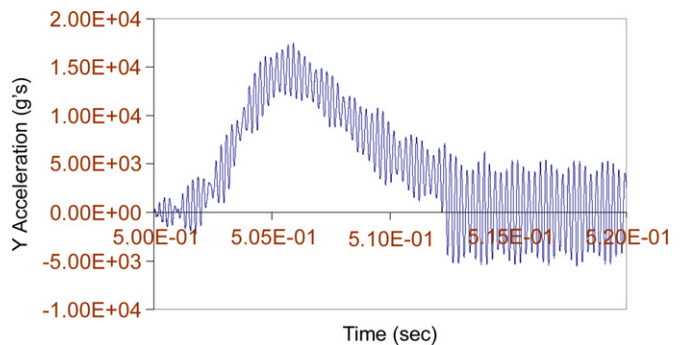


Fig. 17. Filtered axial acceleration for a node on the payload.

thickness of the original steel plate, is used. The acceleration results, Fig. 19, show a significant reduction of magnitude and frequencies of the axial accelerations for the node on the payload. As expected, the acceleration of

the node on the projectile body is practically unchanged when compared to the case of a projectile with a steel supporting plate.

The effect of varying the fiber volume fraction and plate thickness on the transmitted accelerations is explored in the

Table 5
Properties of fiber and matrix

Young’s modulus of fiber (E_f)	3.19E+07 psi
Young’s modulus of matrix (E_m)	5.22E+05 psi
Poisson’s ratio of fiber (ν_f)	0.2
Poisson’s ratio of matrix (ν_m)	0.35
Shear modulus of fiber (G_f)	1.32E+07 psi
Shear modulus of matrix (G_m)	1.92E+05 psi
Density of the fiber (ρ_f)	1.65E-4 lb/in ³
Density of the matrix (ρ_m)	1.12E-4 lb/in ³

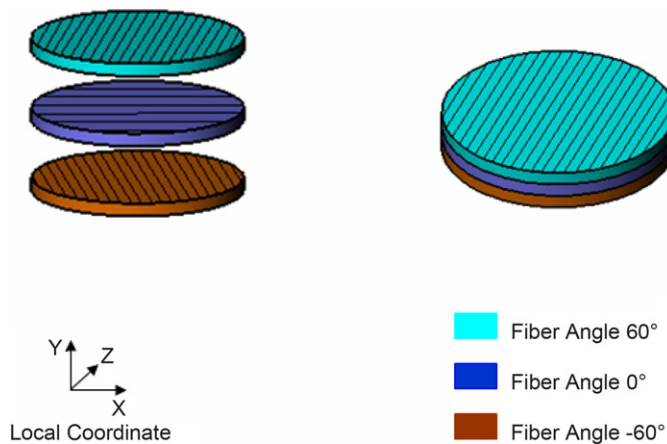


Fig. 18. The three laminae used for the composite laminate.

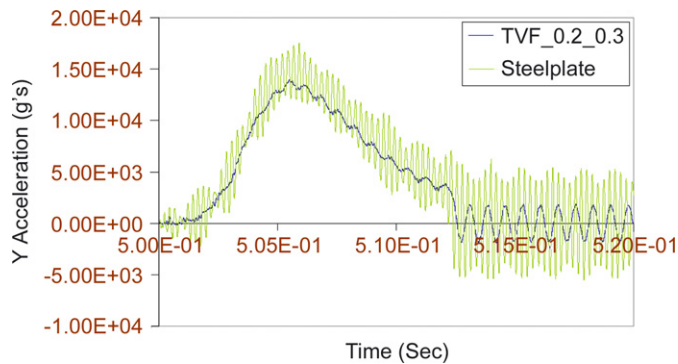


Fig. 19. Filtered y-acceleration for a node on the payload using a 0.2 in steel plate and a plate with 0.2 in thickness and 30% fiber volume fraction respectively.

Table 6
Variation of the plate material properties with fiber volume fraction

Fiber volume fraction (%)	$E_{xx} = E_{zz}$ (psi)	E_{yy} (psi)	ρ (lb/in ³)	G_{xz} (psi)	G_{xy} (psi)	ν_{xy}	ν_{xz}
30	3.8E+06	7.4E+05	0.0502	1.4E+06	1.9E+05	0.023	0.33
40	4.9E+06	8.6E+05	0.0502	1.8E+06	1.9E+05	0.019	0.33
50	6.0E+06	1.0E+06	0.0540	2.3E+06	1.9E+05	0.017	0.32
60	7.2E+06	1.3E+06	0.0540	2.7E+06	1.9E+05	0.017	0.32
70	8.5E+06	1.7E+06	0.0579	3.2E+06	1.9E+05	0.018	0.32

remainder of this section through a parametric study. In this study, the fiber volume fraction is varied from 30% to 70% in steps of 10% while the plate overall thickness is varied from 0.2 to 0.3 in. in steps of 0.05 in. Three laminae of equal thickness are used in each case. Table 6 shows the variation of the material properties as a function of the fiber volume fraction. The table shows that while density and Poisson’s ratio in the $x-z$ direction experience little variation, the values of E_{xx} , E_{yy} , and G_{xz} are more than doubled as the volume fraction increases.

Finite element results for the 15 case studies are presented. Table 7 shows the maximum and minimum filtered axial accelerations outside the gun barrel for the node on the payload. The accelerations on the payload are reduced significantly using a composite plate when compared to the original steel plate, Fig. 19. The acceleration values vary over the considered ranges of composite thickness and fiber volume fraction. No clear pattern is observed to recommend specific composite characteristics over others. The best results are however obtained from the following cases:

- 0.2 in. thickness and 70% fiber volume fraction (1753/–1600 g) and,
- 0.3 in. thickness and 60% fiber volume fraction (1651/–1765 g).

The two above cases correspond to cases that may be difficult to make and maintain control of quality. If such constraints exist, it may be recommended to look at alternatives in Table 7.

Table 8 lists the frequency of the filtered axial acceleration for the 15 case studies. Results show that frequency increases as either plate thickness or fiber volume fraction increases, which is consistent with the change of the plate mechanical characteristics, as shown in Table 6, and the increase of the bending stiffness of the plate, respectively. Table 8 shows over 60% of variation in frequency range between the two extreme cases. The lowest frequencies are obtained from the following cases:

- 0.2 in. thickness and 30% fiber volume fraction (1267 Hz) and,
- 0.2 in. thickness and 40% fiber volume fraction (1400 Hz).

Table 7
Filtered maximum and minimum axial accelerations (*G*) outside the gun barrel

Plate thickness (in.)	Fiber volume fraction (%)				
	30	40	50	60	70
0.2	1869	2109	2023	2350	1753
	-1910	-2229	-2061	-2307	-1600
0.25	1837	19449	1883	2166	1964
	-1719	-19429	-1821	-2265	-1575
0.3	2123	19719	2190	1651	2431
	-2076	-1989	-2153	-1765	-2340

Table 8
Frequency of filtered accelerations (Hz) outside the gun barrel

Plate thickness (in.)	Fiber volume fraction (%)				
	30	40	50	60	70
0.2	1267	1400	1433	1500	1533
0.25	1600	1667	1733	1767	1800
0.3	1833	1900	1933	2000	2067

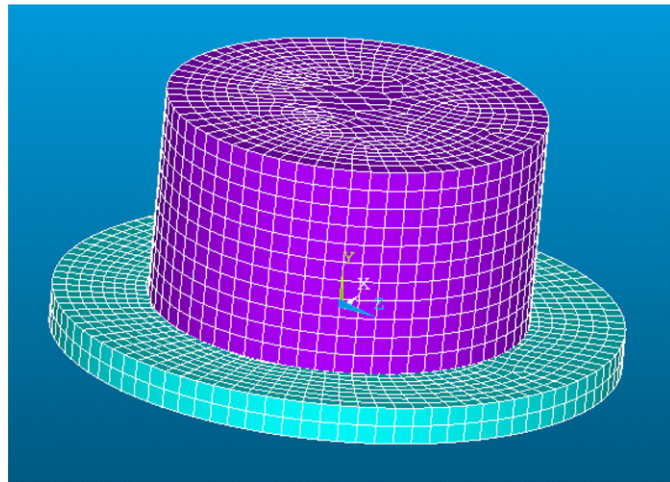


Fig. 20. Model used for modal analysis of the payload and the plate (0.2 in thickness and 30% fiber volume fraction) only.

The above results can lead to the recommendation that relatively thin composite plates with lower natural frequency may be a more attractive alternative as long as stresses are within design limits. To verify that the above results depend on the flexibility of the gun as well as the mass and geometry of the projectile, a modal analysis is conducted for the payload and the plate (0.2 in. thickness and 30% fiber volume fraction) only. The outer edges of the plate are completely fixed as shown in Fig. 20. The first ten natural frequencies of this system are listed in Table 9. Comparison of the results show that modal results of simulating the gun and projectile are significantly below

Table 9
Natural frequencies of the payload and the plate (0.2 in. thickness and 30% fiber volume fraction) only

Mode number	Frequency (Hz)
1	2049
2	2368
3	2568
4	8181
5	8916
6	10,439
7	33,648
8	33,808
9	36,377
10	36,826

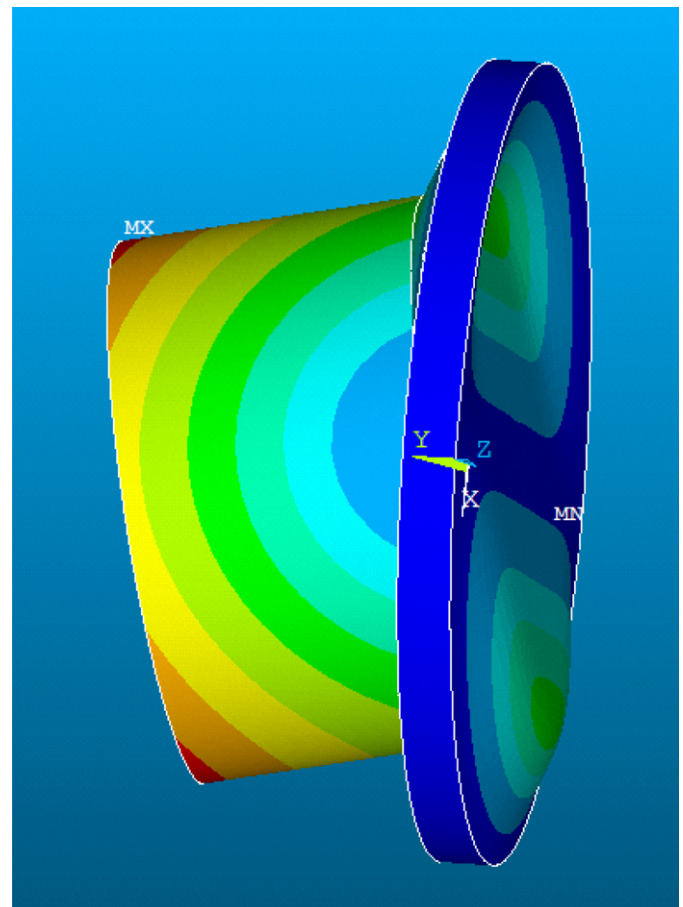


Fig. 21. Mode shape for the first mode of the payload and the plate (0.2 in thickness and 30% fiber volume fraction) only.

those of the plate and the payload only. Fig. 21 shows the mode shape of the first frequency of the plate and payload (Table 10).

5. Conclusions

Components within a projectile are subject to severe shock loadings during and immediately after a gun launch.

Table 10
Equivalent SI units

	US units	SI units equivalent
Length	1 inch	0.0254 m
Weight	1 Pound	0.4535 kg
Temperature	1 F	(5/9)*(1 F-32) °C
Acceleration	1 in/s ²	0.0254 m/s ²
Specific weight	1 lbf/in ³	273386.3 N/m ³
Young's modulus	1 psi	6,894.75 N/m ²
Density	1 lb/in ³	27,679.9 kg/m ³

Extensive experimental tests of such components can be prohibitively expensive. This paper presents an approach to model the gun-launch dynamic interaction between a projectile body, its internal components, and the gun barrel. The proposed approach includes the effects of the flexibility of the gun barrel, friction between the projectile and the gun, and flexibility of a mounting plate for an electronic payload. While FEM displacement and velocity results for nodes on projectile were satisfactory, there is a need for filtering the FEM acceleration data as the acceleration results contained higher level of noise than what is observed in corresponding test data. A filtering approach based on modal analysis of the projectile is used in this research.

A parametric study is also conducted to explore the possibility of using a composite plate to support an electronic payload. In this study, fiber volume fraction and thickness are varied. All cases in the parametric study experience marked reduction in magnitude and frequency of payload accelerations when compared to the results found when using a steel plate of the same size. Simulation results also show that the composite plates with lower fiber volume fraction and thickness provide the lowest frequency of the acceleration response after the gun muzzle exit. This observation can be useful in reducing the possibility of low-cycle fatigue failure of electronic components.

The current model is computationally intensive. Methods for reduced computational time, without sacrificing accuracy, are currently under investigation. Experimental verification of shock transmission through composite plates is needed for further tuning of the FEMs. Future studies may include effects of gun recoil on the model and fiber orientation angles of the laminae.

Acknowledgments

The authors would like to acknowledge the help of Dr. Donald Carlucci, Mr. Matt Hawkswell, and Mr. Michael Hollis (US Army TACOM-ARDEC) for their continued support and numerous discussions. The authors would also like to thank Mr. Ami Frydman, US Army Research Laboratory, for suggesting this research topic and interacting with the authors. Funding for the work is provided by ARL through the Soldier's Future Force Electronics Reliability and Survivability Technology

Program (Soldier FERST), cooperative agreement number DAAD19-03-2-0007.

Appendix A. Elastic properties of composite laminates

Elastic properties of the composite lamina are estimated using Rule of Mixture's equations following [17]. Young's Modulus of the composite lamina along the fiber direction is calculated using the following equation:

$$E_{11} = E_f V_f + E_m V_m. \quad (\text{A.1})$$

Transverse modulus and shear modulus of the composite lamina are calculated as follows:

$$E_{22} = \frac{E_f E_m}{E_f V_m + E_m V_f}, \quad (\text{A.2})$$

$$G_{12} = \frac{G_f G_m}{G_f V_m + G_m V_f}. \quad (\text{A.3})$$

Major and minor Poisson's ratios of the composite lamina are calculated using the following formulas:

$$v_{12} = v_f V_f + v_m V_m, \quad (\text{A.4})$$

$$v_{21} = \frac{E_{22}}{E_{11}} v_{12}. \quad (\text{A.5})$$

Fig. 18 shows the stacking sequence of the laminae in the laminate. The material properties of the laminate are found by calculating extensional stiffness matrix $[A]$ of the laminate,

$$[A] = \begin{bmatrix} A_{11} & A_{12} & A_{16} \\ A_{12} & A_{22} & A_{26} \\ A_{16} & A_{26} & A_{66} \end{bmatrix}. \quad (\text{A.6})$$

$[A]$ is calculated using the following formula:

$$[A] = [\bar{Q}]_{+60^\circ}(h_0 - h_1) + [\bar{Q}]_{0^\circ}(h_1 - h_2) + [\bar{Q}]_{-60^\circ}(h_2 - h_3), \quad (\text{A.7})$$

where $[\bar{Q}]_\theta$ is the stiffness matrix for the individual lamina, which is defined as

$$[\bar{Q}]_\theta = \begin{bmatrix} \bar{Q}_{11} & \bar{Q}_{12} & \bar{Q}_{16} \\ \bar{Q}_{12} & \bar{Q}_{22} & \bar{Q}_{26} \\ \bar{Q}_{16} & \bar{Q}_{26} & \bar{Q}_{66} \end{bmatrix}. \quad (\text{A.8})$$

Elements of $[\bar{Q}]_\theta$ can be calculated using the following formulas [17]:

$$\bar{Q}_{11} = Q_{11} \cos^4 \theta + 2(Q_{12} + 2Q_{66})\sin^2 \theta \cos^2 \theta + Q_{22} \sin^4 \theta, \quad (\text{A.9})$$

$$\bar{Q}_{12} = Q_{12}(\sin^4 \theta + \cos^4 \theta) + (Q_{11} + Q_{22} - 4Q_{66})\sin^2 \theta \cos^2 \theta, \quad (\text{A.10})$$

$$\bar{Q}_{22} = Q_{11} \sin^4 \theta + 2(Q_{12} + 2Q_{66})\sin^2 \theta \cos^2 \theta + Q_{22} \cos^4 \theta, \quad (\text{A.11})$$

$$\begin{aligned} \bar{Q}_{16} = & (Q_{11} - Q_{12} - 2Q_{66}) \sin \theta \cos^3 \theta \\ & + (Q_{12} - Q_{22} + 2Q_{66}) \sin^3 \theta \cos \theta, \end{aligned} \quad (\text{A.12})$$

$$\begin{aligned} \bar{Q}_{26} = & (Q_{11} - Q_{12} - 2Q_{66}) \sin^3 \theta \cos \theta \\ & + (Q_{12} - Q_{22} + 2Q_{66}) \sin \theta \cos^3 \theta, \end{aligned} \quad (\text{A.13})$$

$$\begin{aligned} \bar{Q}_{66} = & (Q_{11} + Q_{12} - 2Q_{12} - 2Q_{66}) \sin^2 \theta \cos^2 \theta \\ & + Q_{66} (\sin^4 \theta + \cos^4 \theta), \end{aligned} \quad (\text{A.14})$$

where θ is the fiber orientation angle of the lamina

$$Q_{11} = \frac{E_{11}}{1 - \nu_{12}\nu_{21}},$$

$$Q_{22} = \frac{E_{22}}{1 - \nu_{12}\nu_{21}},$$

$$Q_{12} = Q_{21} = \frac{\nu_{12}E_{22}}{1 - \nu_{12}\nu_{21}},$$

$$Q_{66} = G_{12}.$$

The properties of the laminate are:

– In-plane Young's modulus:

$$E_{xx} = E_{zz} = \frac{A_{11}^2 - A_{22}^2}{(h_0 + h_3)A_{11}}. \quad (\text{A.15})$$

– In-plane Poisson's ratio:

$$\nu_{xz} = \frac{A_{12}}{A_{11}}. \quad (\text{A.16})$$

– In-plane shear modulus:

$$G_{xz} = \frac{A_{11} - A_{12}}{2(h_0 + h_3)}. \quad (\text{A.17})$$

– Transverse modulus:

$$E_{yy} = E_{22}. \quad (\text{A.18})$$

– Poisson's ratio in the transverse direction:

$$\nu_{xy} = \nu_{21}. \quad (\text{A.19})$$

– Shear modulus in the transverse direction:

$$G_{xy} = G_m. \quad (\text{A.20})$$

– Density of the Composite Laminate:

$$\rho_c = \rho_f V_f + \rho_m V_m. \quad (\text{A.21})$$

References

- [1] Chowdhury M, Frydman AMR, Cordes J, Reinhardt L, Carlucci D. 3-D Finite-element gun launch simulation of a surrogate Excalibur 155 mm guided artillery projectile-modeling capabilities and its implications. In: Flis WJ, Scott B, editors. 22nd international symposium on ballistics, Vancouver, Canada. Lancaster, Pennsylvania: DEStech Publications, Inc.; 2005. p. 259–67.
- [2] Cordes JA, Carlucci D, Jafar R. Dynamics of a simplified 155-MM projectile. Army TACOM-ARDEC (internal report), 2004.
- [3] Heaslip G, Punch J. Analysis of experimental shock and impact response data of a printed wire board. Electronic Photonic Packing, Electrical Systems Photonic Des Nanotechnol 2003;3: 125–33.
- [4] Berman M, Hopkins D, Powers B, Minnicino M. Numerical and experimental modeling of the transition from transient to quasi-static loading of printed wiring assemblies. In: SEM annual conference and exposition on experimental and applied mechanics. Bethel, CT: Society for Experimental Mechanics, Inc.; 2003.
- [5] Simkins T, Pflagl G, Stilson E. Dynamic strains in a 60 MM gun tube: an experimental study. J Sound Vib 1993;168:549–57.
- [6] Hopkins DA, Wilkerson S. Analysis of a balanced breech system for the M1A1 main gun system using finite element techniques. In: Computers in engineering, Proceedings of the international conference and exhibit, ASME, New York, 1994. p. 519–32.
- [7] Hollis M. Use of finite element stress analysis in the design of a tank-cannon-launched training projectile. In: Computers in engineering, Proceedings of the international conference and exhibit, ASME, New York, 1994. p. 533–44.
- [8] Kessler S, Spearing S. Design, analysis and manufacture of a high-g composite fuselage structure. In: Whitney J, editor. Proceedings of the American society of composites. Dayton, OH: American Society for Composites; 2000. p. 945–52.
- [9] Petersen E. AGS barrel motion during firing: experimental and modeling results. In: Proceedings of the 2005 SEM annual conference and exposition on experimental and applied mechanics. Bethel, CT: Society for Experimental Mechanics, Inc.; 2005. p. 1125–32.
- [10] Tzeng J, Sun W. Dynamic response of cantilevered rail guns attributed to projectile/gun interaction—theory. IEEE Trans Magn 2007;43(1):207–13.
- [11] Steffen Jr. V, Rade D, Inman D. Using passive techniques for vibration damping in mechanical systems. In: Proceedings of the 25th international conference on noise and vibration engineering, ISMA. Belgium: Katholieke Universiteit Leuven; 2000. p. 363–70.
- [12] Trindade M. Optimization of sandwich/multilayer viscoelastic composite structure for vibration damping. In: Chakrabarti SK, editor. Proceedings of the international conference on offshore mechanics and arctic engineering, OMAE, vol. 3. New York, NY: American Society of Mechanical Engineering; 2001. p. 257–64.
- [13] Cordes J, Vega J, Carlucci D, Chaplin R. Design accelerations for the Army's excalibur projectile. US Army Technical Report, ARAET-TR-05008, 2005.
- [14] LS-DYNA Keyword User's Manual version 970. Livermore software technology corporation, 2003.
- [15] Gibson R. Principles of composite material mechanics. New York: McGraw-Hill; 1994. p. 190–269.
- [16] Ayyaswamy A, Sridharala S, Trabia M, O'Toole B, Liu Q, Chowdhury M. Characterization of electronic board material properties under impact loading. Seattle, WA: ASME IMECE; 2007.
- [17] Mallik P. Fiber reinforced composites. New York: Marcel Dekker; 1993. 91–200.

NO. OF
COPIES ORGANIZATION

1 DEFENSE TECHNICAL
(PDF INFORMATION CTR
only) DTIC OCA
8725 JOHN J KINGMAN RD
STE 0944
FORT BELVOIR VA 22060-6218

1 US ARMY RSRCH DEV &
ENGRG CMD
SYSTEMS OF SYSTEMS
INTEGRATION
AMSRD SS T
6000 6TH ST STE 100
FORT BELVOIR VA 22060-5608

1 DIRECTOR
US ARMY RESEARCH LAB
IMNE ALC IMS
2800 POWDER MILL RD
ADELPHI MD 20783-1197

1 DIRECTOR
US ARMY RESEARCH LAB
AMSRD ARL CI OK TL
2800 POWDER MILL RD
ADELPHI MD 20783-1197

1 DIRECTOR
US ARMY RESEARCH LAB
AMSRD ARL CI OK T
2800 POWDER MILL RD
ADELPHI MD 20783-1197

ABERDEEN PROVING GROUND

1 DIR USARL
AMSRD ARL CI OK TP (BLDG 4600)

NO. OF
COPIES ORGANIZATION

1 DIRECTOR
US ARMY RSRCH LAB
AMSRD ARL SE DE
R ATKINSON
2800 POWDER MILL RD
ADELPHI MD 20783-1197

15 DIRECTOR
US ARMY RSRCH LAB
AMSRD ARL WM MB (ALC)
A ABRAHAMIAN
M BERMAN
M CHOWDHURY (CPS 10)
A FRYDMAN
R KARGUS
T LI
2800 POWDER MILL RD
ADELPHI MD 20783-1197

1 COMMANDER
US ARMY MATRL CMND
AMXMI INT
9301 CHAPEK RD
FORT BELVOIR VA 22060-5527

1 COMMANDER
US ARMY TACOM ARDEC
AMSRD AAR EM
J HEDDERICH
PICATINNY ARSENAL NJ 07806-5000

1 COMMANDER
US ARMY TACOM ARDEC
AMSRD AAR EMT
B MACHAK
PICATINNY ARSENAL NJ 07806-5000

5 COMMANDER
US ARMY TACOM ARDEC
AMSRD AAR AEP E
D CARLUCCI
K LAUGHLIN
S GROESCHLER
J LEE
J VEGA
BLDG 94
PICATINNY ARSENAL NJ 07806-5000

1 COMMANDER
US ARMY TACOM ARDEC
AMSRD AAR AEM J
G FLEMING
PICATINNY ARSENAL NJ 07806-5000

NO. OF
COPIES ORGANIZATION

2 COMMANDER
US ARMY TACOM ARDEC
AMSRD AAR EBM
R CARR
W SHARPE
BLDG 1
PICATINNY ARSENAL NJ 07806-5000

3 COMMANDER
US ARMY TACOM ARDEC
SFAE AMO MAS LC
R DARCY
R JOINSON
D RIGOGLIOSO
BLDG 354
PICATINNY ARSENAL NJ 07806-5000

2 COMMANDER
US ARMY TACOM ARDEC
AMSRD AAR AEM L
P DONADIA
D VO
BLDG 65 S
PICATINNY ARSENAL NJ 07806-5000

8 COMMANDER
US ARMY TACOM ARDEC
AMSRD AAR AEM
M PALATHINGUL
A VELLA
L MANOLE
S MUSALLI
M LUCIANO
E LOGSDEN
T LOUZEIRO
J LUTZ
PICATINNY ARSENAL NJ 07806-5000

2 COMMANDER
US ARMY TACOM ARDEC
AMSRD AAR AEE P
D KAPOOR
S KERWIEN
PICATINNY ARSENAL NJ 07806-5000

1 COMMANDER
US ARMY TACOM ARDEC
AMSRD AAR AIP
M LOS
PICATINNY ARSENAL NJ 07806-5000

NO. OF
COPIES ORGANIZATION

2 SFSJM CDL
AMMUN TEAM
AMSIO SMT
R CRAWFORD
W HARRIS
1 ROCK ISLAND ARSENAL
ROCK ISLAND IL 61299-6000

12 BENET LABS
AMSTA AR CCB
M SOJA
E KATHE
G SPENCER
P WHEELER
S KRUPSKI
J VASILAKIS
G FRIAR
AMSTA CCB R
S SOPOK
E HYLAND
D CRAYON
R DILLON
G VIGILANTE
WATERVLIET NY 12189-4050

1 US ARMY TARDEC
AMSRD TAR R
D TEMPLETON
6501 E 11 MILE RD MS 263
WARREN MI 48397-5000

1 PEO GROUND COMBAT SYS
SFAE GCS BCT/MS 325
M RYZYI
6501 ELEVEN MILE RD
WARREN MI 48397-5000

2 USA RDECOM
AMSRD AMR AE F T
F RUMPF
J CHANG
BLDG 488 B247
REDSTONE ARSENAL AL 35898

1 USA RDECOM
AMSRD AMR AE F A
M ROGERS
BLDG 4488 B244
REDSTONE ARSENAL AL 35898

NO. OF
COPIES ORGANIZATION

3 USA RDECOM
AMSRD AMR AE F M
K BHANSALI
G LIU
R MCFARLAND
BLDG 4488 B272
REDSTONE ARSENAL AL 35898

4 US ARMY RSRCH OFC
J PRATER
D STEPP
D KISEROW
W MULLINS
PO BOX 12211
RESEARCH TRIANGLE PARK NC
27709-2211

1 OFC OF NAVAL RSRCH
J CHRISTODOULOU
ONR CODE 332
800 N QUINCY ST
ARLINGTON VA 22217-5600

1 COMMANDER
US ARMY TACOM ARDEC
AMSTA AR CCL B
J MIDDLETON
BLDG 65N
PICATINNY ARSENAL NJ 07806-5000

1 COMMANDER
US ARMY TACOM ARDEC
ASIC PRGM INTEGRATION OFC
J RESCH
BLDG 1
PICATINNY ARSENAL NJ 07806-5000

1 COMMANDER
US ARMY TACOM ARDEC
AMSRD AAR AEW M(D)
M MINISI
BLDG 65 N
PICATINNY ARSENAL NJ 07806-5000

1 US ARMY TACOM ARDEC
AMSRD AR CCL C
S SPICKERT-FULTON
BLDG 65 N
PICATINNY ARSENAL NJ 07806-5000

<u>NO. OF COPIES</u>	<u>ORGANIZATION</u>
1	US ARMY ARDEC AMSRD AAR AEM I D CONWAY BLDG 65 N PICATINNY ARSENAL NJ 07806-5000
4	PM ARMS SFAE AMO MAS SMC R KOWALSKI F HANZL P RIGGS M BULTER BLDG 354 PICATINNY ARSENAL NJ 07806-5000
1	PM ARMS SFAE AMO MAS MC BLDG 354 PICATINNY ARSENAL NJ 07806-5000
8	FORT SILL FIELD ARTILLERY S COFFMAN G LEMONS B LEWIS J HALL D CARLSON R NELSON C NIEDERHAUSER FDIC USAFAC D BROWN BUILDING 700 (KNOX HALL) FORT SILL OK 73503
1	FORT SILL FIELD ARTILLERY HQ US ARMY FIRES CTR R HADDOCK 640 MCBRIDE AVE FORT SILL OK 73503
1	FORT SILL FIELD ARTILLERY USAFAS BLDG 3040 G DURHAM FORT SILL OK 73503-5600
1	FORT SILL FIELD ARTILLERY COUNTER STRIKE TASK FORCE H ELLIS FORT SILL OK 73503-7500
1	FORT SILL FIELD ARTILLERY TSM CANNON J TANZI FORT SILL OK 73503

<u>NO. OF COPIES</u>	<u>ORGANIZATION</u>
1	FORT SILL FIELD ARTILLERY TCM FSC3 J HAITHCOCK 569 CRUIKSHANK CIR FORT SILL OK 73503
2	DARPA S WAX L CHRISTODOULOU 3701 N FAIRFAX DR ARLINGTON VA 22203-1714
1	DIRECTOR NGIC IANG TMT 2055 BOULDERS RD CHARLOTTESVILLE VA 22091-5391
3	INST FOR ADVANCD TECH H FAIR I MCNAB S BLESS 3925 W BRAKER LN AUSTIN TX 78759-5316
1	ALLIANT TECHSYSTEMS INC R DOHRN MN11 1428 600 SECOND ST NE HOPKINS MN 55343
2	ALLIANT TECHSYSTEMS INC C AAKHUS D KAMDAR MN11 2830 600 SECOND ST NE HOPKINS MN 55343
1	ATK M JANTSCHER MN07 LW54 4700 NATHAN LN N PLYMOUTH MN 55442
1	ALLIANT TECHSYSTEMS INC R BECKER MN11 2626 5050 LINCOLN DR EDINA MN 55340-1097

<u>NO. OF COPIES</u>	<u>ORGANIZATION</u>
2	ATK LAKE CITY SMALL CALIBER AMMUN LAKE CITY ARMY AMMUN PLANT K ENLOW D MANSFIELD PO BOX 1000 INDEPENDENCE MO 64051-1000
1	ATK LAKE CITY LAKE CITY ARMY AMMUN PLANT SMALL CALIBER AMMUN J WESTBROOK MO10 003 PO BOX 1000 INDEPENDENCE MO 64051-1000
3	DIRECTOR LLNL R CHRISTENSEN S DETERESA F MAGNESS PO BOX 808 LIVERMORE CA 94550
1	ARMTEC DEFENSE PRODUCTS S DYER 85 901 AVE 53 PO BOX 848 COACHELLA CA 92236
3	PACIFIC NORTHWEST LAB M SMITH G VAN ARSDALE R SHIPPELL PO BOX 999 RICHLAND WA 99352
1	CUSTOM ANALYTICAL ENG SYS INC A ALEXANDER 13000 TENSOR LANE NE FLINTSTONE MD 21530
3	ALLIANT TECHSYSTEMS INC J CONDON E LYNAM J GERHARD WV01 16 STATE RT 956 PO BOX 210 ROCKET CENTER WV 26726-0210

<u>NO. OF COPIES</u>	<u>ORGANIZATION</u>
2	GENERAL DYNAMICS OTS FLINCHBAUGH DIV K LINDE G KURZIK PO BOX 127 RED LION PA 17356
1	ARROW TECH ASSOC 1233 SHELBURNE RD STE D8 SOUTH BURLINGTON VT 05403-7700
1	UNIV OF CINCINNATI DEPT OF AEROSPACE ENG & ENG MECHANICS A TABIEI 722 RHODES HALL PO BOX 210070 CINCINNATI OH 45221-0070
4	UNIV OF DELAWARE CTR OF COMPOSITE MTRLS J GILLESPIE S LOPATNIKOV S YARLAGADDA S ADVANI 215 COMPOSITES MANUFAC SCI LAB NEWARK DE 19716
1	UNIV OF DELAWARE CTR OF COMPOSITE MTRLS M SANTARE 126 SPENCER LAB NEWARK DE 19716
1	DEPT OF MECH ENG UNIV OF NEVADA LAS VEGAS M TRABIA 4505 MARYLAND PKWY BOX 454027 LAS VEGAS NV 89154-4027
1	PENN STATE UNIV C BAKIS 212 EARTH ENGR SCIENCES BLDG UNIVERSITY PARK PA 16802

NO. OF
COPIES ORGANIZATION

ABERDEEN PROVING GROUND

1 US ARMY ATC
CSTE DTC AT AD I
W FRAZER
400 COLLERAN RD
APG MD 21005-5059

63 DIR USARL
AMSRD ARL CI
AMSRD ARL O AP EG FI
M ADAMSON
AMSRD ARL WM
J SMITH
S KARNA
J MCCAULEY
P PLOSTINS
T WRIGHT
AMSRD ARL WM B
M ZOLTOSKI
J NEWILL
AMSRD ARL WM BA
D LYON
AMSRD ARL WM BC
P WEINACHT
AMSRD ARL WM BD
B FORCH
P CONROY
AMSRD ARL WM BF
W OBERLE
AMSRD ARL WM M
S MCKNIGHT
J BEATTY
R DOWDING
AMSRD ARL WM MA
M VANLANDINGHAM
AMSRD ARL WM MB
J BENDER
T BOGETTI
L BURTON
R CARTER
W DE ROSSET
W DRYSDALE
R EMERSON
D HOPKINS
R KASTE
L KECSKES
E KLIER
H MAUPIN
M MINNICINO
B POWERS
D SNOHA

NO. OF
COPIES ORGANIZATION

J SOUTH
J SWAB
J TZENG
AMSRD ARL WM MC
E CHIN
J ADAMS
B CHEESEMAN
J MONTGOMERY
AMSRD ARL WM MD
M MAHER
W SPURGEON
AMSRD ARL WM T
P BAKER
AMSRD ARL WM TA
S SCHOENFELD
N GNIAZDOWSKI
D HACKBARTH
C HOPPEL
AMSRD ARL WM TB
J COLBURN
R GUPTA
B MCANDREW
R SKAGGS
AMSRD ARL WM TC
G BOYCE
R COATES
K KIMSEY
L MAGNESS
B SCHUSTER
B SORENSEN
R SUMMERS
B WALTERS
AMSRD ARL WM TD
T BJERKE
D CASEM
T WEERASOORIYA
AMSRD ARL WM TE
B RINGERS

INTENTIONALLY LEFT BLANK.